High-order harmonic generation and above-threshold ionization in H: Calculations using expansions over field-free state-specific wave functions

S. Dionissopoulou, Th. Mercouris, A. Lyras,* Y. Komninos, and C. A. Nicolaides
Theoretical and Physical Chemistry Institute, National Hellenic Research Foundation, 48, Vas. Constantinou Avenue, 11635 Athens, Greece
(Received 14 February 1994; revised manuscript received 31 October 1994)

We have computed the above-threshold ionization and the emitted harmonic spectra of H interacting with short laser pulses, with photon energies ranging from 1.16 to 5.44 eV and with peak intensities ranging from 6×10^{13} to 7×10^{14} W/cm^2, by solving the time-dependent Schrödinger equation (TDSE). The method of solution involves the expansion of the time-dependent wave function $\Psi(\vec{r},t)$ over the exact wave functions of the discrete and the continuous spectrum, computed numerically, and the subsequent integration of the resulting coupled first-order differential equations by a Taylor series expansion technique. This state-specific approach (SSA) to the solution of the TDSE allows systematic understanding of convergence as a function of the number and type of the field-free states for each value of the laser frequency (ω) and peak intensity (I_0). For example, the method allows practical numerical study of the degree of participation of high (n,l) $(l=0,1,\ldots,n-1)$ Rydberg, as well as of high-energy scattering states for each partial wave. For the harmonic spectra, comparisons are made between the results obtained by the SSA and those obtained in recent years by a number of researchers from the application of finite-difference grid methods. As regards economy, a general observation is that in the SSA the necessary number of partial waves is smaller than that required in the grid methods. Predictions are made for the case of $\hbar\omega=2$ eV, $I_0=2\times10^{14}$ W/cm^2, in the context of a study of the effect of the pulse shape on the harmonic-generation spectrum. It is shown that the number of harmonics and the appearance of the plateau depend on the duration of the peak intensity.

PACS number(s): 42.50.Hz, 32.80.Rm

I. INTRODUCTION

There is growing interest in the nonperturbative calculation of the spectrum of high-order harmonic generation (HOHG) occurring during the interaction of an atom with a short laser pulse of high intensity [1–10]. In order to deal with this problem rigorously, one must solve the time-dependent Schrödinger equation (TDSE) for the system "atom plus laser pulse," and then use the solution $\Psi(\vec{r},t)$ for the calculation of the harmonic spectrum, which is proportional to [1–3]

$$|d(\omega)|^2=\left|\frac{1}{T_2-T_1}\int_{T_1}^{T_2}dt\, e^{-i\omega t}d(t)\right|^2 . \quad (1)$$

The quantity $d(\omega)$ is the Fourier transform of the induced time-dependent dipole $d(t)$, determined by

$$d(t)=\langle\Psi(\vec{r},t)|\vec{d}|\Psi(\vec{r},t)\rangle . \quad (2)$$

The operator $\vec{d}$ may have a number of forms. The usual ones are the length, velocity, and acceleration, with appropriate frequency factors multiplying expression (1). Based on a number of arguments and results on one-electron atoms [4,6,7,9,10] and on models [11], the authors of these papers suggest the superiority of the acceleration form.

The existing calculations on HOHG of real atoms have applied the so-called "grid method," whereby the TDSE is integrated directly on a grid of space-time points, for the computation of the wave function of only one electron moving either in a purely Coulomb potential (hydrogen atom), or in a mean-field local potential (closed-shell noble gases) [1–10]. In conjunction with the use of supercomputers, this approach has already produced much information on the phenomenon of HOHG and on other properties resulting from the nonlinear response of atoms to strong laser pulses. However, it is still not possible for the grid method to go beyond the single-electron approximation or to deal efficiently with multideterminantal zeroth-order states. Furthermore, even for the hydrogen atom, convergence difficulties appear as the intensity increases or the photon energy decreases. For example, in a systematic study and analysis, Krause, Schafer, and Kulander [6] computed the HOHG for H interacting with laser pulses of wavelength 1064 nm and of peak intensities ranging from 2×10^{13}–1×10^{14} W/cm^2. For the latter case, "converged results become extremely difficult to obtain," in spite of the impressive capacity of the vectorized code. The causes and the implications of this limitation were discussed by the authors [6].

It is the purpose of this paper to present results on the above-threshold ionization (ATI) spectra and on HOHG for the hydrogen atom for a number of cases, from an approach that brings in the characteristics of the real

*Present address: Department of Physics, University of Ioannina, P.O. Box 1186, 45110 Ioannina, Greece.

discrete and continuous spectrum via the use of state-specific wave functions. One advantage of this approach to the solution of the TDSE, demonstrated here, is efficiency, good convergence, and an immediate understanding as to the significance of the discrete and scattering states that are included in the calculation in a modular way. A more general advantage, demonstrated elsewhere [12] where the details of the method are presented, is that it allows the quantitative treatment of polyelectronic atoms regardless of their structure and the character of their field-free spectrum.

In Sec. II we give the essential equations used in the calculations of the state-specific approach (SSA). Since the functions representing the discrete and the scattering states are calculated numerically, the bottleneck as to the on-shell singularity for the continuum-continuum dipole matrix elements had to be solved. The solution is given in Ref. [12]. In Sec. III we present a series of results for intensities in the range $6\times10^{13}-7\times10^{14}$ W/cm^2 and for photon energies in the range 1.16–5.44 eV. These are compared with the available results from grid methods [4–7].

II. METHOD: EXPANSION BASED ON STATE-SPECIFIC WAVE FUNCTIONS

The approach which we chose for solving the TDSE starts with the textbook case of expanding $\Psi(\vec{r},t)$ over the field-free stationary states of the spectrum under study with time-dependent coefficients:

$$\Psi(\vec{r},t)=\sum_{i,n}\alpha_i(n,t)\Phi_{n,i}+\sum_i\int b_i(E,t)\Phi_{E,i}dE \ . \tag{3}$$

$\Phi_{n,i}$ are the bound states and $\Phi_{E,i}$ are the energy-normalized scattering wave functions. The index i signifies the orbital angular momentum channel. Substituting Eq. (3) into the TDSE results in a system of coupled first-order differential equations whose solution produces the coefficients α_i and b_i. Knowledge of α_i and b_i allows immediately the calculation of a variety of observables.

The total Hamiltonian is taken in the form

$$H_{\rm tot}=H_{\rm at}+i\vec{A}(t)\cdot\vec{\nabla} \ , \tag{4}$$

where, for reasons of computational convenience in dealing with the continuum-continuum dipole matrix elements using numerical functions, the velocity form of the interaction has been adopted [12]. The vector potential $\vec{A}(t)$ is related to the electric-field amplitude by

$$\vec{E}(t)=-\frac{d}{dt}\vec{A}(t)=\vec{E}_0f(t)\sin\omega t \ , \tag{5}$$

where $f(t)$ is the function for the shape of the pulse. In our calculations the light is linearly polarized and the magnetic quantum number is set to zero for all channels.

The features that distinguish the SSA and make it general as well as efficient are that the wave functions Φ_n and Φ_E are state specific and that the free-orbital functions are obtained numerically for each partial wave. As has been argued before (e.g., [13], and references therein), implementing theories of a variety of atomic or molecular processes in terms of state-specific wave functions, instead of functions that are produced by diagonalization of the Hamiltonian over a single large basis set, offers important conceptual and computational advantages, since the function space for each wave function is optimized separately and since the free-electron function is obtained numerically in the field of the term-dependent core. In this way, the resulting wave functions are compact yet accurate, have a one-to-one correspondence with real states, no information-loosing discretization of the electronic continuum is necessary, and the inclusion selectively of electron correlation and of multiply excited states in the discrete or the continuous spectrum is straightforward.

For the present problem involving hydrogen, the state-specific discrete and scattering functions are obtained exactly from the numerical solution of the hydrogenic Schrödinger equation. In this way, the convergence of the method and the physics of the phenomenon under study can be understood, given the laser characteristics, as a function of the number and the type of the field-free states entering Eq. (3).

Form of the dipole operator for the calculation of $d(t)$

In order to compute $d(t)$ of Eq. (2) for linearly polarized light, we chose the acceleration form

$$d(t)=d_A(t)=\left\langle\Psi(\vec{r},t)\left|E_0f(t)\sin(\omega t)-\frac{z}{r^3}\right|\Psi(\vec{r},t)\right\rangle \ . \tag{6}$$

This choice was made for reasons of convenience in the calculation of the continuum-continuum matrix elements with numerical functions, and of direct comparison with the existing results from the grid approach.

We take this opportunity to comment on the choice of the appropriate form in general, i.e., in the case of polyelectronic atoms. In the one-electron case, the use of the acceleration form for the computation of the harmonic spectrum has the following advantage: By weighting the inner part of the wave function, this form excludes to a good degree possible errors in $\Psi(\vec{r},t)$ coming from the outer region when the atom is ionized. When the grid method is applied, its results have shown that this leads to the reduction of background in the spectrum [6,7,11].

On the other hand, for multielectron atoms the choice of the appropriate form is less obvious. As is well known, it is rarely possible to calculate oscillator strengths for transitions in multielectron systems with all three forms of the dipole operator and obtain good agreement among them and with experiment [14]. Furthermore, the acceleration form is considered to be the least reliable for processes involving the valence electrons since it emphasizes the small-r values of a numerical multielectron wave function, and the value of the corresponding approximate transition matrix element deviates from the accurate one significantly.

In other words, consider the matrix element (2) and write $d(t)$ as

$$\sum_k \sum_m \langle \alpha_k(t)\Phi_k|\vec{d}|\alpha_m(t)\Phi_m\rangle = d(t) , \quad (7)$$

where the indices k and m run over the complete set of discrete and scattering stationary states. It is obvious that one factor determining the value of each term is the magnitude of the time-dependent coefficients, and this depends on the ionization probability for the laser pulse of interest. The other major factor is the accuracy of each matrix element. For example, suppose that we consider high-order transitions to the ground state Φ_0 only. The corresponding matrix elements are

$$\sum_m \alpha_0^*(t)\alpha_m(t)\langle \Phi_0|\vec{d}|\Phi_m\rangle , \quad (8)$$

where the Φ_m represent continuum states. For a polyelectronic atom where the laser pulse has excited one or more valence electrons, the results of the computation of the N-electron integrals in Eq. (8) will be less reliable when the acceleration form is used than when the length or the velocity form are used, unless very accurate wave functions for Φ_0 and Φ_m are used [14].

III. RESULTS AND COMPARISON WITH PREVIOUS WORK

We now turn to the discussion of specific results obtained for H, the common testing ground of each new approach. Except for the case of $\hbar\omega=2$ eV, $I_0=2\times10^{14}$ W/cm^2, these results were obtained with a pulse shape $f(t)$ of the form [5,6]

$$f(t)=\begin{cases} t/T_r , & 0\le t\le T_r \\ 1 , & T_r\le t\le T_f , \end{cases} \quad (9)$$

where T_r is the rise time of the pulse and T_f is the time at which the constant intensity part ends. This form is particularly convenient for the Taylor series expansion method, which we introduced [12] for the solution of the TDSE. It should be kept in mind that the details of the pulse shape will not affect significantly the qualitative characteristics of the harmonic spectra.

The above shape covers the cases of relatively long pulses. On the other hand, in order to check the possibility of producing higher harmonics with very short pulses, we also did a case ($\hbar\omega=2$ eV, $I_0=2\times10^{14}$ W/cm^2) where $d(t)$ was evaluated for the full duration of the pulse (see case G).

The Fourier transform, [Eq. (1)] of the time-dependent dipole [Eq. (6)] was performed with a standard fast-Fourier-transform (FFT) routine [15]. We used as input the values of $d(t)$ during the last 4–8 cycles of the pulse. In most cases presented here, the rise time was $T_r=5T$ and the pulse ended at $T_f=20T$. In this way the sampled values of the dipole are not affected by transient effects due to the rise of the pulse intensity.

$\Psi(\vec{r},t)$ and $d(t)$ [Eq. (6)] were calculated at intervals ranging from $T/800$ to $T/2048$ to ensure that even the highest harmonics produced could be resolved.

A number of cases were examined in order to check the convergence properties of the SSA, to explore trends, and to compare with available results from the approach that computes $\Psi(\vec{r},t)$ using grid methods [4–7]. The ATI spectra were obtained by computing

$$\frac{dP_\varepsilon(t)}{d\varepsilon}=|b(\varepsilon,t)|^2 . \quad (10)$$

Case A. $\hbar\omega=1.16$ eV, ($\lambda=10640$ Å), $I_0=1\times10^{14}$ W/cm^2

We start with this case because it has been used as a stringent test of the accuracy and economy of the SSA. As we already mentioned in the Introduction, Krause, Schafer, and Kulander [6] have recently reported calculations of HOHG showing that convergence is extremely difficult to obtain. In fact, they estimated that the acceleration spectra—which were identified as the most reliable—have converged only to within an order of magnitude (Ref. [6], p. 5008).

Our results are shown in Figs. 1–4, where HG as well as ATI spectra are shown. Convergence was tested by increasing systematically the number of hydrogenic bound states (n and l) and of the scattering states (E and l). Figures 1–4 correspond to calculations where the required number of bound states has stabilized at $n=20$, $l=14$, and the continuum extends to $E=70$ eV in steps of 0.054 eV. Thus what we show reflects the convergence as a function of the number of partial waves in the continuum. Figs. 1 and 3 correspond to $l=20$ and Figs. 2 and 4, our final results, to $l=30$. In the former case, the number of coupled equations is 27 411 and in the latter 40 371. In either case, the numerical algorithm [12] was very stable. It is clear that the spectra from the two calculations ($l=20$ and $l=30$) are essentially the same, signifying that convergence has already been obtained at $l=20$.

As regards the harmonic spectra, when comparison is made between the SSA and the grid results (Fig. 16 of Ref. [6]), similarities as well as differences are observed. The forms of the spectra from the two types of calcula-

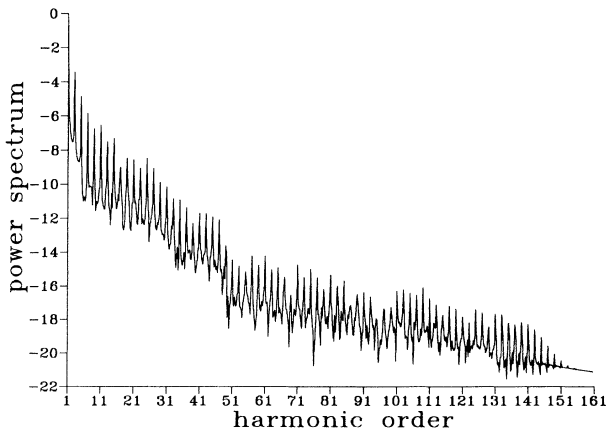

FIG. 1. Harmonic response ($\log_{10}|d(\omega)|^2$ [Eq. (1) from Eq. (6) divided by ω^4]), of H versus harmonic order. The field frequency is $\hbar\omega=1.16$ eV ($\lambda=10\,640$ Å) and the peak intensity is $I_0=1\times10^{14}$ W/cm^2. The number of partial waves in the continuum goes up to $l=20$. In this as well as in all figures, the base of the logarithm is 10.

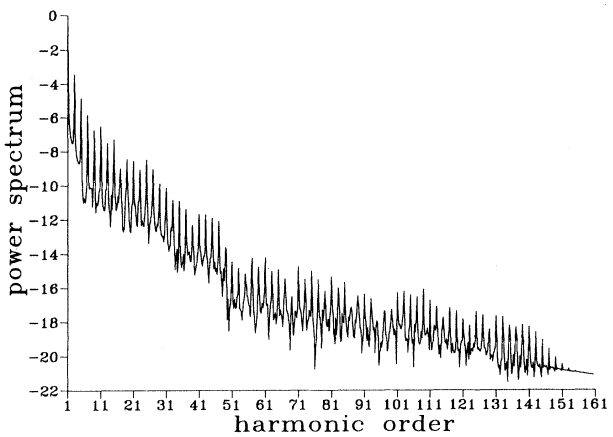

FIG. 2. As in Fig. 1 with partial waves in the continuum up to $l=30$.

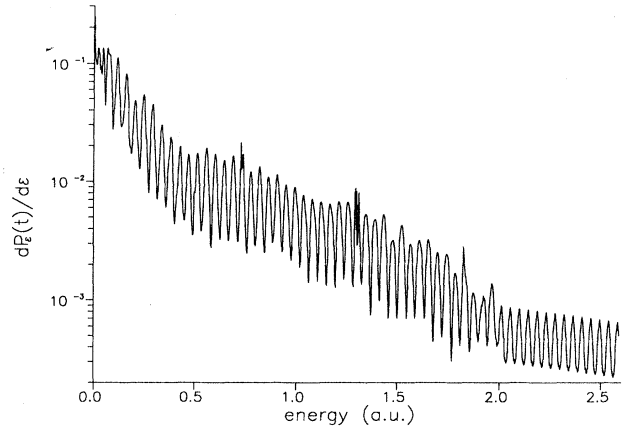

FIG. 4. As in Fig. 3 with partial waves in the continuum up to $l=30$.

tion are similar (acceleration formulas). Such similarities are observed for the appearance of the position of the cutoff, the intensity of the peaks, and the role of the background (compare Fig. 16(a) of Ref. [6] with our Fig. 2).

Case B. $\hbar\omega=5.44$ *eV,* ($\lambda=2280$ *Å*), $I_0=1.75\times10^{14}$ *W/cm*^{2}

This is the case treated by DeVries [5]. His results show the appearance of harmonic generation through the 23rd harmonic. Our results (Fig. 5) show an emitted radiation only up to the 7th harmonic, with no plateau or cutoff.

Case C. $\hbar\omega=5.0$ *eV,* ($\lambda=2480$ *Å*), $I_0=7\times10^{14}$ *W/cm*^{2}

For this case the expansion (3) consisted of 195 discrete hydrogen functions (up to $n=20$, $l=14$) and 13 608 scattering functions (648 energies per l channel and up to 21 l channels) with an energy spacing 0.004 a.u., thus covering energies up to 2.59 a.u. above the ionization threshold. The results plotted in Fig. 6 show appreciable amplitudes for harmonics up to the 9th, which however are many orders of magnitude weaker than the fundamental. No sign of a plateau is present despite the high intensity of the pulse. This is in accord with all the experimental evidence accumulated so far, clearly supporting the conclusion that longer wavelengths are more efficient in the generation of high-order harmonics [16]. However, our results are at least partly in conflict with recently published results [7] that show that for 5-eV photons and with $I_0=7\times10^{14}$ W/cm^2, a long plateau extending from the 9th to the 25th harmonic is formed

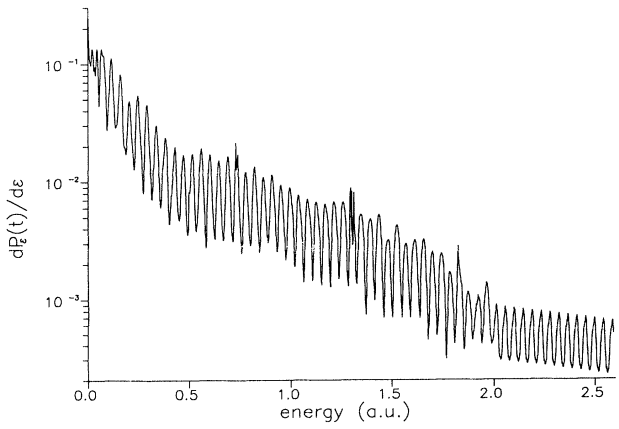

FIG. 3. ATI spectrum ($dP_\varepsilon(t)/d\varepsilon$ [Eq. (10)] in logarithmic scale) of H as a function of photoelectron energy (in a.u.). The field frequency and the peak intensity are as those of Fig. 1. The number of partial waves in the continuum goes up to $l=20$.

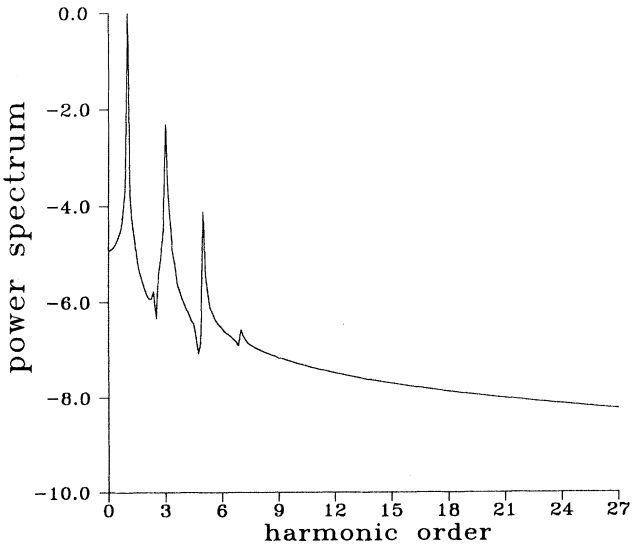

FIG. 5. Harmonic response (in logarithmic scale) of H versus harmonic order with $\hbar\omega=5.44$ eV and $I_0=1.75\times10^{14}$ W/cm^2.

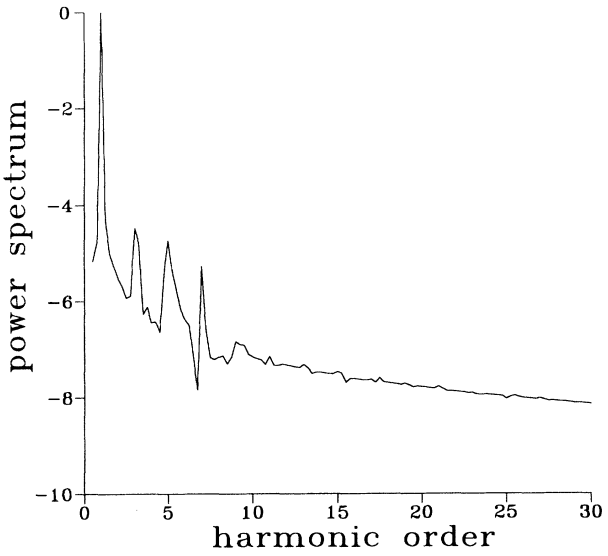

FIG. 6. Harmonic spectrum for H at $\hbar\omega=5.0$ eV and laser intensity of $I_0=7\times10^{14}$ W/cm^2.

while the harmonic spectrum shows appreciable amplitude up to the 35th order. We have performed all the routine tests to ensure that our results are converged and no numerical artifacts influence the outcome of the calculation. In fact, we could obtain nearly identical results with half the number of bound states and continuum one-channels included in the expansion.

Case D. $\hbar\omega=5$ eV, ($\lambda=2480$ Å), $I_0=2.42\times10^{14}$ W/cm^2

This is the case treated by LaGattuta [4]. Our results for the ATI spectrum (Fig. 7) agree with his. There is also agreement between the results of the two calculations for the ionization rate ($\approx2.6\times10^{14}$ sec^{-1}). On the other hand, there is a difference in the HG spectra. Both calculations produced three peaks (our Fig. 8; Fig. 8 of Ref. [4]). However, in our spectrum the intensity of the peaks is decreasing with harmonic order whereas in the spectrum of [4], the second peak is the highest.

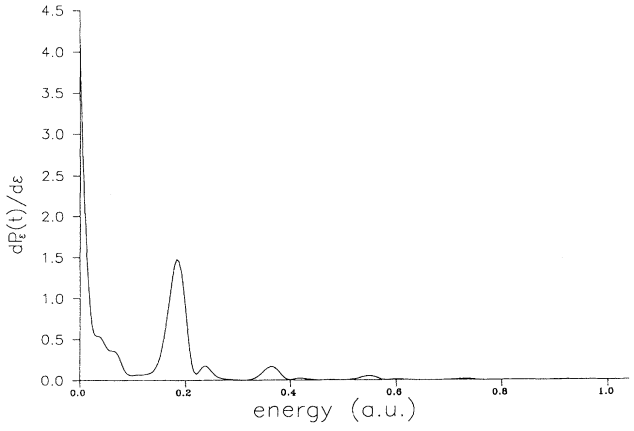

FIG. 7. ATI spectrum (in linear scale) of H for $\hbar\omega=5.0$ eV and $I_0=2.42\times10^{14}$ W/cm^2.

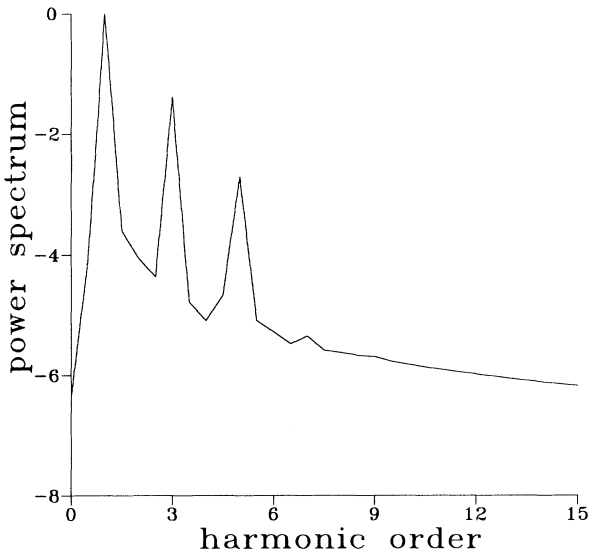

FIG. 8. Harmonic spectrum for H at $\hbar\omega=5.0$ eV and laser intensity of $I_0=2.42\times10^{14}$ W/cm^2.

Case E. $\hbar\omega=3$ eV, ($\lambda=4143$ Å), $I_0=8\times10^{13}$ W/cm^2, $I_0=2\times10^{14}$ W/cm^2

The results for two peak intensities are shown in Figs. 9 and 10. First, in Fig. 9, a peak intensity of $I_0=8\times10^{13}$ W/cm^2 was used. A clearly perturbative picture emerges with harmonics formed only up to the 5th order. Compared with the results in Figs. 6 and 8, it is confirmed that the longer wavelength is definitely more efficient in harmonic production. This is further corroborated by the case where the peak intensity is increased to $I_0=2\times10^{14}$ W/cm^2 (Fig. 10). The 7th harmonic emerges strongly from the background, and the heights of succes-

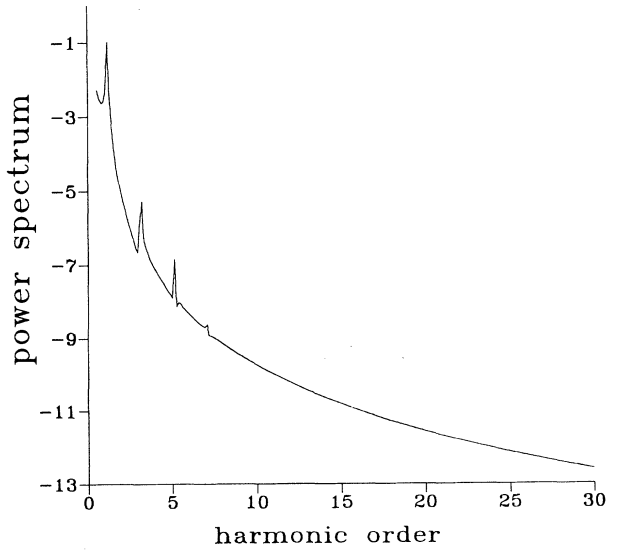

FIG. 9. Harmonic spectrum ($\log_{10}|d(\omega)|^2$ [Eq. (1) from Eq. (6) divided by ω^2]) for H at $\hbar\omega=3.0$ eV and $I_0=8\times10^{13}$ W/cm^2.

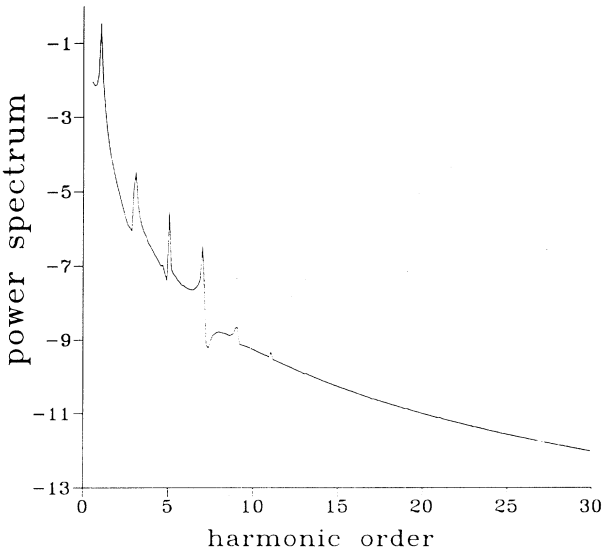

FIG. 10. As in Fig. 9 but for $I_0=2\times10^{14}$ W/cm^2.

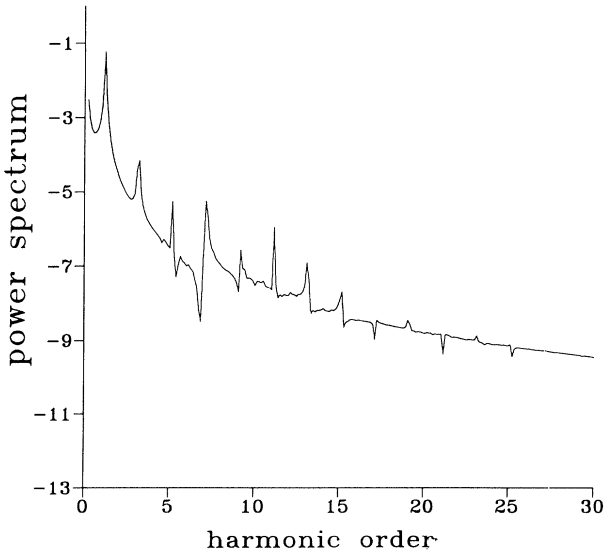

FIG. 12. As in Fig. 11 but for $I_0=8\times10^{13}$ W/cm^2.

sive orders of harmonics tend to converge to a band of only two orders of magnitude, a precursor of plateau formation.

Case F. $\hbar\omega=2$ eV, ($\lambda=6078$ Å), $I_0=6\times10^{13}$ W/cm^2, 8×10^{13} W/cm^2, 1.2×10^{14} W/cm^2

In order to exhibit the nonperturbative response of the atomic system under long-wavelength, high-intensity excitation, we have further reduced the pump frequency to $\omega=0.075$ a.u. ($\hbar\omega=2$ eV). This photon energy lies in the range produced by state of the art laser systems (like the Ti-sapphire type) that can deliver very high intensities in very short pulses (less than 100 fsec). It is therefore expected that interesting experimental results will keep on coming at this photon energy.

In Fig. 11, results are shown for $I_0=6\times10^{13}$ W/cm^2. At this intensity, relatively low for H, the harmonic spectrum already exhibits significant departure from the perturbative response encountered in Figs. 6 and 9. The strength of the 3rd and 5th harmonics is comparable. The same holds true for a second group of harmonics, from the 7th to the 13th, which seem to form a short "plateau" region. By further increasing the intensity to $I_0=8\times10^{13}$ W/cm^2 (Fig. 12), the plateau formation covers the range from the 5th to the 15th harmonic. The perturbative behavior is now limited only to the 3rd harmonic. The final set of results obtained with $I_0=1.2\times10^{14}$ W/cm^2 (Fig. 13) does not show any appre-

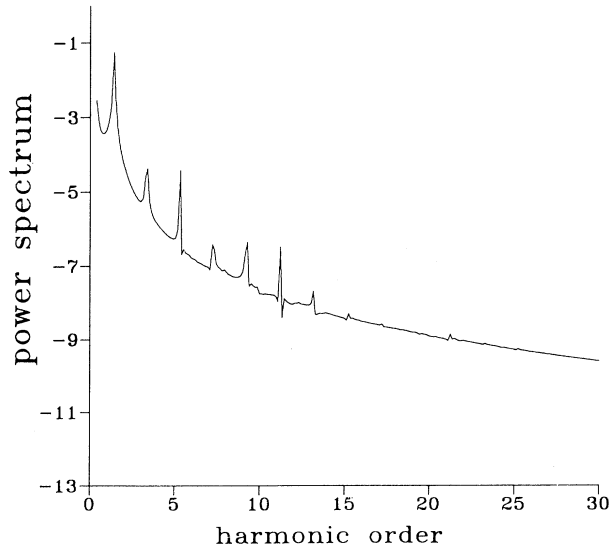

FIG. 11. Harmonic spectrum [$|d(\omega)|^2$ divided by ω^2] for H at $\hbar\omega=2.0$ eV and $I_0=6\times10^{13}$ W/cm^2.

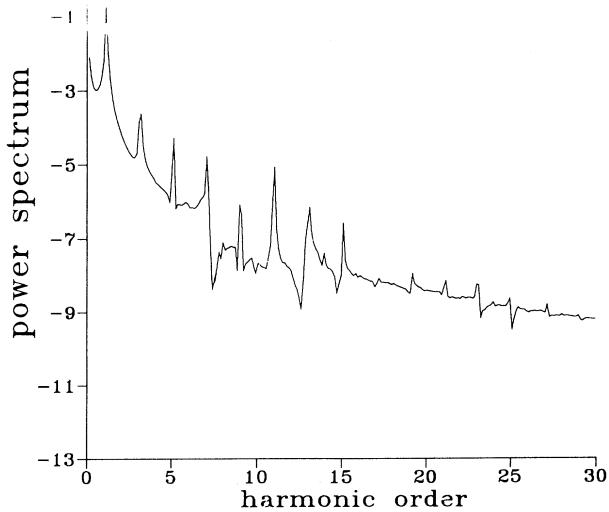

FIG. 13. As in Fig. 11 but for $I_0=1.2\times10^{14}$ W/cm^2.

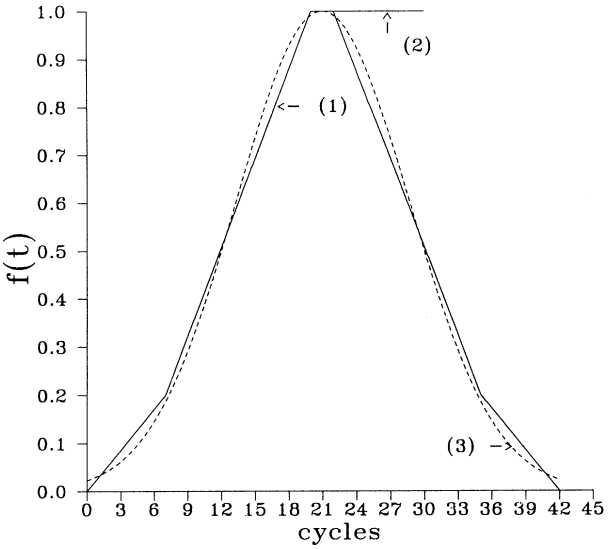

FIG. 14. Temporal pulse shape used in case G [curve (1)]. The solid-line curve (1) consists of a rising time (as well as a fall time) composed of two linear portions (with a duration of 7 and 13 cycles, respectively) and of a part of a constant peak intensity with a duration of 2 cycles. The dashed-line curve (3) corresponds to a Gaussian temporal pulse shape with full width at half maximum 18 cycles=40 fsec. The curve (2) indicates a pulse where the part of constant peak intensity is longer.

ciable increase in the extent of the plateau. This could probably be due to the increase in ionization as the peak intensity increases. As a result, electrons are quickly removed from the vicinity of the nucleus, and the harmonic emission is not enhanced appreciably despite the considerable increase of the driving power. This last set of results has converged to below an order of magnitude at the positions of the harmonic peaks and the background.

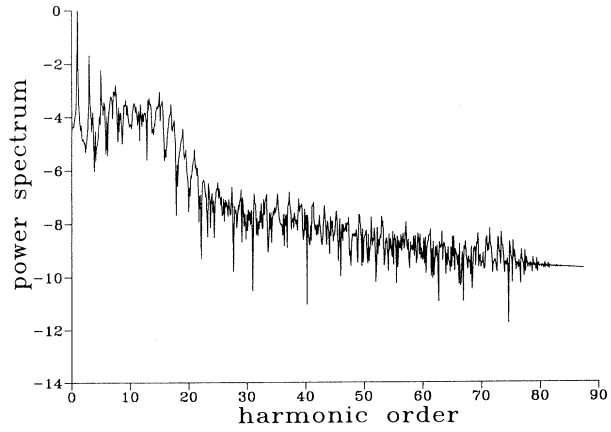

FIG. 15. Harmonic response (in logarithmic scale) of H versus harmonic order with $\hbar\omega=2$ eV and $I_0=2\times10^{14}$ W/cm^2. This spectrum was obtained from the full duration of the pulse [curve (1) in Fig. 14].

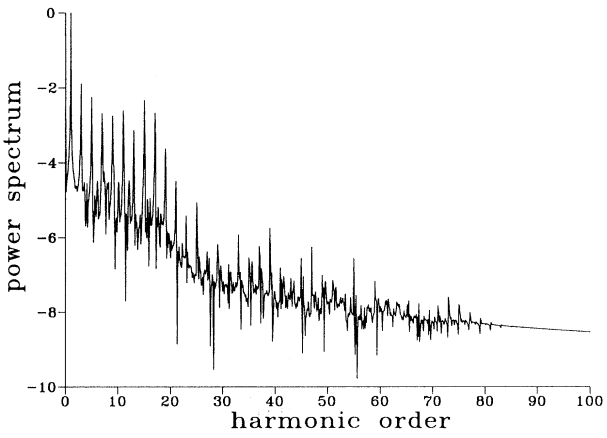

FIG. 16. As in Fig. 15 but for a longer part of peak intensity [curve (2) in Fig. 14].

Case G. $\hbar\omega=2$ eV, ($\lambda=6078$ Å), $I_0=2\times10^{14}$ W/cm^2

In this case we tested the efficiency of producing high-order harmonics in very short intense pulses. We used the full duration of the pulse for the calculation of $d(t)$ [Eq. (6)]. The shape of the pulse used in this case as well as a Gaussian-type pulse of the same full width at half maximum (18 cycles = 40 fsec) are shown in Fig. 14. The results of Fig. 15 show clearly only three harmonics with a tendency toward the formation of a plateau and a cutoff. Evidently, the system feels the peak intensity only for a very short time and cannot respond in terms of many harmonics.

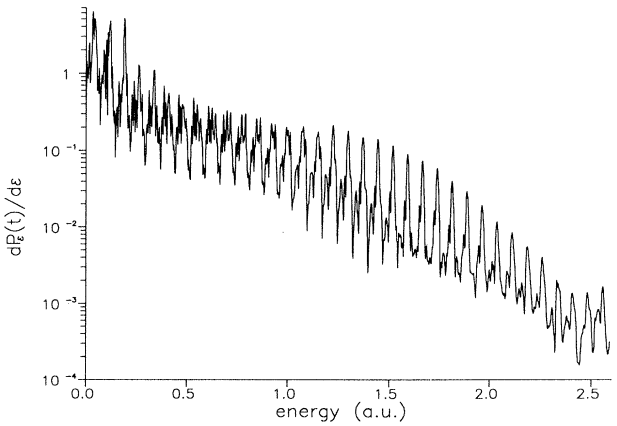

FIG. 17. ATI spectrum (in logarithmic scale) of H for $\hbar\omega=2.0$ eV and $I_0=2\times10^{14}$ W/cm^2. This spectrum was obtained at the end of the pulse [curve (1) in Fig. 14].

By extending the duration of the peak intensity [see curve (2) in Fig. 14], harmonics up to the 19th are observed (Fig. 16). In this spectrum one can detect a plateau between the 7th and the 17th harmonics. Also, a cutoff appears at the energy of 3.17 U_p+I_p [18], where U_p is the ponderomotive potential and I_p is the ionization potential. The ATI spectrum is given in Fig. 17. Here, there is no previous theoretical or experimental information with which to compare.

IV. CONCLUSION

In order to compute the ATI spectra [via Eq. (10)] and the high harmonics via the Fourier transform of the time-dependent dipole moment [Eqs. (1) and (2)] of real atoms, an alternative approach to the grid methods [1–10] for the calculation of $\Psi(t)$ has been applied. The reported results refer to the H atom excited by a variety of strong laser pulses. The method converged well for the most difficult case reported in the literature [6], i.e., for $\lambda=1064$ nm and $I_0=1\times10^{14}$ W/cm^2, while consistently showing efficient convergence for a number of other cases.

The present results suggest that the strategy of solving the TDSE via the use of the state-specific expansion of Eq. (3), where the stationary wave functions are obtained by an advanced method allowing for a faithful representation of the unperturbed states of the discrete and the continuous spectrum, is suitable for the treatment of a number of problems (see also Refs. [12,17]). For polyelectronic systems, the rate of convergence and the degree of transparency from the viewpoint of physics will depend on the quality of the wave functions Φ_n and Φ_E and on the number of states entering Eq. (3). The present application to the hydrogen atom offered the opportunity of using the optimal Φ_n and Φ_E, i.e., the exact functions. We found that as regards convergence, the contribution to $\Psi(t)$ comes mainly from the continuous spectrum. Since the high-lying discrete states of a polyelectronic atom are hydrogenlike, it follows that, apart from special situations of valence-Rydberg interactions, the level of accuracy in the calculation of $\Psi(t)$ for a polyelectronic atom will depend mainly on how accurately the contribution of the free-electron spectrum has been accounted for.

ACKNOWLEDGMENT

We thank Professor P. Lambropoulos for sending us unpublished results by H. Xu and P. Lambropoulos on the HOHG for $\hbar\omega=2$ eV, 5 eV, $I_0=2\times10^{13}$ W/cm^2.

[1] For reviews and discussions, see J. H. Eberly, J. Javanainen, and K. Rcazewski, Phys. Rep. **204**, 331 (1991), and the articles by A. L.'Huillier *et al.*, K. C. Kulander *et al.* and J. H. Eberly *et al.* in, *Atoms in Intense Laser Fields,* edited by M. Gavrila (Academic, New York, 1992).

[2] K. C. Kulander and B. W. Shore, Phys. Rev. Lett. **62**, 524 (1989); J. Opt. Soc. Am. B **7**, 502 (1990); K. C. Kulander, Phys. Rev. A **35**, 445 (1987).

[3] J. H. Eberly, Q. Su, J. Javanainen, K. C. Kulander, B. W. Shore, and L. Roso-Franco, J. Mod. Opt. **36**, 829 (1989).

[4] K. J. LaGattuta, Phys. Rev. A **41**, 5110 (1990).

[5] P. L. DeVries, J. Opt. Soc. Am. B **7**, 517 (1990).

[6] J. L. Krause, K. J. Schafer, and K. C. Kulander, Phys. Rev. A **45**, 4998 (1992).

[7] T.-F. Jiang and S.-I. Chu, Phys. Rev. A **46**, 7322 (1992).

[8] H. Xu, X. Tang, and P. Lambropoulos, Phys. Rev. A **46**, R 2255 (1992).

[9] K. J. LaGattuta, J. Mod. Opt. **39**, 1181 (1992); J. H. Eberly and M. V. Fedorov, Phys. Rev. A **45**, 4706 (1992).

[10] H. Xu, Z. Phys. D **28**, 27 (1993).

[11] K. Burnett, V. C. Reed, J. Cooper, and P. L. Knight, Phys. Rev. A **45**, 3347 (1992).

[12] Th. Mercouris, Y. Komninos, S. Dionissopoulou, and C. A. Nicolaides, Phys. Rev. A **50**, 4109 (1994).

[13] Th. Mercouris and C. A. Nicolaides, Phys. Rev. A **48**, 628 (1993).

[14] C. A. Nicolaides and D. R. Beck, Chem. Phys. Lett. **35**, 202 (1975).

[15] W. H. Press, B. P. Flannery, S. A. Teukolsky, and W. T. Vetterling, *Numerical Recipes* (Cambridge University Press, Cambridge, England, 1986), Chap. 12.

[16] Ph. Balcou, C. Cornaggia, A. S. L. Gomes, L. A. Lompre, and A. L'Huillier, J. Phys. B **25**, 4467 (1992).

[17] Th. Mercouris, I. D. Petsalakis, P. Valtazanos, and C. A. Nicolaides, J. Phys. B **27**, L519 (1994).

[18] J. L. Krause, K. J. Schafer, and K. C. Kulander, Phys. Rev. Lett. **68**, 3535 (1992); M. Lewenstein, Ph. Balcou, M. Yu. Ivanov, Anne L'Huillier, and P. B. Corkum, Phys. Rev. A **49**, 2117 (1994).